

# Learning distant cause and effect using only local and immediate credit assignment

David Rawlinson  
Incubator 491  
dave@agi.io

Abdelrahman Ahmed  
Incubator 491  
abdel@agi.io

Gideon Kowadlo  
Incubator 491  
gideon@agi.io

May 29, 2019

## Abstract

We present a recurrent neural network memory that uses sparse coding to create a combinatoric encoding of sequential inputs. Using several examples, we show that the network can associate distant causes and effects in a discrete stochastic process, predict partially-observable higher-order sequences, and enable a DQN agent to navigate a maze by giving it memory. The network uses only biologically-plausible, local and immediate credit assignment. Memory requirements are typically one order of magnitude less than existing LSTM, GRU and autoregressive feed-forward sequence learning models.

The most significant limitation of the memory is generalization to unseen input sequences. We explore this limitation by measuring next-word prediction perplexity on the Penn Treebank dataset.

## 1. Introduction

Researchers have been unable to find a biological equivalent to the deep error backpropagation used widely in artificial neural networks (O’Reilly, 1996; Luo et al., 2017). This presents a credit assignment problem: How do biological neurons determine the influence of a synapse on an error that may occur many layers distant, or many steps in the future? The answer to this question is of practical significance because it may yield alternative, superior learning rules. Existing biologically-plausible approaches to the distant credit assignment problem have noticeable performance limitations when compared to *implausible* learning rules (Balduzzi et al., 2015; Bengio et al., 2015). In this paper, we hope to overcome some of these limitations while preserving biological plausibility, using the approach of combinatoric sparse coding.

## 1.1. Sequence learning

To date, the most successful architectures for sequence learning are Recurrent Neural Networks (RNNs) and autoregressive, feed-forward networks (Oord et al., 2016). Truncated Back-Propagation Through Time (BPTT) (Sutskever, 2013) unrolls the state of a RNN over a fixed number of time steps  $t$ , allowing errors to be assigned to the relevant synaptic weights. The network cannot be trained to exploit causes earlier than  $t$  time-steps.

Autoregressive, feed-forward networks utilize a fixed moving window of  $t$  most recent inputs, that are processed simultaneously through several layers. Error gradients are back-propagated through the layers. Like truncated BPTT, context more distant than  $t$  steps cannot be utilized. Techniques such as dilated convolutions allow  $t$  to be quite large (100 steps or more).

Credit assignment in the above methods is widely believed to be biologically implausible due to backpropagation through time and layers.

Credit assignment over time can also be achieved by forward-propagating derivatives of hidden states and outputs with respect to each synaptic weight. Real-Time Recurrent Learning (RTRL) (Williams & Zipser, 1995) is an instance of this concept, but is rarely used in practice due to the difficulty of maintaining viable derivatives.

## 1.2. Gated memory cells

In ordinary RNNs, iterative partial derivative updates are likely to produce vanishing or exploding gradients. Gated memory layers such as Long-Short-Term-Memory (LSTM) (Hochreiter & Schmidhuber, 1997) and Gated Recurrent Units (GRUs) (Chung et al., 2014) mitigate this problem by creating a more robustly differentiable relationship between memory state, gate operations and outputs. Using gated memory cells, causes and effects may be successfully associated despite separation by hundreds of steps. However, the memory requirements of gated memory layers are much larger than BPTT with ordinary RNNs, due to the

---

requirement to train many gate-control parameters.

### 1.3. Practical requirements

How much context do we actually need for human-like performance? Let’s take natural language modelling as an example. (Chelba et al., 2013) showed that on the Billion Word benchmark, an LSTM  $n$ -gram model where  $n = 13$  was as good as LSTMs with access to longer history. In fact, even with simple smoothed  $n$ -gram language models such as Kneser-Ney (Ney et al., 1994), longer histories do not yield practical advantage, in part because the additional higher-order context is unlikely to generalize well, especially in smaller datasets.

Recent work by (Bai et al., 2018) showed that in general, feed-forward autoregressive models with dilated convolutions tend to outperform RNNs. They also showed that even where very long term context was definitely necessary, RNNs could not exploit it. The encoding of context is at least as important as the amount of context.

So in summary, for competitive performance on natural language benchmarks it is likely only necessary to perform credit assignment over context of, perhaps, 100 steps. Since natural languages are tailored to human capabilities, this may be indicative of general human limits. Psychological studies of human problem-solving suggest that we work with relatively simple mental simulations of short sequences of highly abstracted features (Khemlani et al., 2013).

### 1.4. Biologically plausible criteria

We adopted the following criteria for biological plausibility:

- Only local credit assignment. No back-propagation of errors between cell-layers
- No synaptic memory beyond the current and/or next step
- No time-travel, making use of past or future inputs or hidden states

The computational capabilities of single-layer networks are very limited, especially in comparison to two-layer networks. Biological neurons perform “dendrite computation”, involving integration and nonlinearities within dendrite subtrees (Guerguiev et al., 2017). This is computationally equivalent to 2 or 3 typical artificial neural network layers. For this reason we allow ourselves to use error backpropagation across two ANN layers, under the assumption that this could approximate dendrite computation within a single biological cell layer, and training signals inside cells.

### 1.5. Memorization approach

Gated memory layers learn to selectively remember important features. If we can only back-propagate errors across 2 or 3 time steps, how can we learn to retain data that won’t be useful for tens or hundreds of steps?

One option is to simply remember everything, which means we could use any past observation to predict a future effect. At first glance this seems impractical, even if we were to limit observations to one hundred steps; but (Hawkins & Ahmad, 2016) showed that a form of sparse coding can allow networks to have vast representational capacity, by virtue of all the *combinations* in which cells can be active.

Sparse coding simply means that most cells have zero value - they are inactive (Olshausen & Field, 1997). In Hawkins & Ahmad’s HTM model, the few active cells jointly represent not just the current input, but previous inputs as well. This is achieved by applying local inhibition to groups of cells - within each group, different cells fire in response to different sequential contexts. Since a long context is encoded in the current state without filtering for salience, we will refer to this strategy as the memorization approach.

## 2. Method

We will attempt to implement the memorization approach to sparse sequence encoding using a more conventional RNN, trained with stochastic gradient descent. For convenience we will refer to our approach as recurrent sparse memory (RSM). It is derived from the sparse autoencoders developed by Makhzani and Frey (Makhzani & Frey, 2013; 2015). In their algorithm, a fixed top- $k$  sparsity is applied; sparseness is the only nonlinearity.

An autoencoder learns to reconstruct the current external input  $x^A(t)$  through a bottleneck. To make an autoencoder learn transitions, we instead train it to generate a prediction  $\hat{x}^A(t)$  of the next external input  $x^A(t + 1)$  using a mean square error loss.

To allow the network to use previous inputs as context for the prediction, we add a recurrent input  $x^B$ , containing a copy of layer cell activity from the previous step.

Cells within the layer are organized into groups. All cells in a group share the same (optionally convolutional) weights for external input  $A$ . Each cell has its own set of fully-connected weights for recurrent input  $B$ . The parameter  $m$  specifies the number of groups. Parameter  $n$  is the number of cells in each group.

#### 2.0.1. THEORY OF OPERATION

The network described above is similar to a conventional recurrent layer. However, we add an inhibition term  $\phi$  (de-

fined below) that causes cells to become selectively active in particular sequential contexts. The same observation in different contexts is then represented by a different set of active cells.

When a group of cells responds strongly to an input  $\mathbf{x}^A$ , the least inhibited cell in the group becomes active. Inhibition due to the refractory period ensures that all cells in a group learn unique contexts in which to fire. Fixed sparsity ensures that cells and groups learn to be active in a huge variety of unique combinations. Each combination of cells encodes not just the current input, but a long history of prior inputs as well. As in (Hawkins & Ahmad, 2016), the memory can represent many long histories using the current set of active cells, in effect learning a higher-order representation of these sequences.

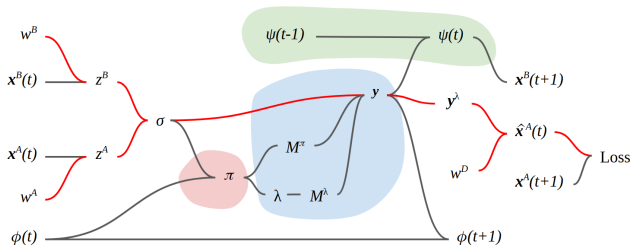


Figure 1: RSM diagram. RSM is trained to generate predictions  $\hat{\mathbf{x}}^A(t)$  of its next external input  $\mathbf{x}^A(t+1)$ . Red lines show how this loss propagates to the learned parameters  $w^A$ ,  $w^B$  and  $w^D$ . The model is a standard recurrent network with the addition of inhibition (red patch), rank-based sparse masking (blue patch) and integration & normalization of recurrent input (green patch).

## 2.0.2. MODEL DETAILS

See figure 1 for an overview of the model. We can calculate the matrix product of inputs and weights as normal for a single ANN layer. Note that each cell has a unique set of recurrent weights  $w^B$ , whereas all cells in a group share the same external input weights  $w^A$ :

$$\mathbf{z}^A = w^A \mathbf{x}^A(t)$$

$$\mathbf{z}^B = w^B \mathbf{x}^B(t)$$

$\sigma_{ij}$  is a matrix of dimension (groups  $\times$  cells) i.e.  $m \times n$ . The weighted sum  $\sigma_{ij}$  of a cell  $j$  in group  $i$  is given by:

$$\sigma_{ij} = z_i^A + z_{ij}^B$$

We shift the weighted sums to positive nonzero values and calculate cell activity  $\pi$  after applying an inhibition term  $\phi$ :

$$\pi_{ij} = (1 - \phi_{ij}(t)) \cdot (\sigma_{ij} - \min(\sigma) + 1)$$

We reduce cell activity  $\pi$  to group activity  $\lambda$  by taking the max value of the cells in each group:

$$\lambda_i = \max(\pi_{i1}, \dots, \pi_{in})$$

The next step is to calculate two sparse binary masks  $M$ .  $M^\pi$  indicates the most active cell in each group.  $M^\lambda$  indicates the most active groups in the layer. We use a function  $\text{topk}(a, b)$  that returns a ‘1’ for the top  $b$  elements in the last dimension of argument  $a$ , and ‘0’ otherwise.

$$M^\pi = \text{topk}(\pi, 1)$$

$$M^\lambda = \text{topk}(\lambda, k)$$

We take the elementwise product of the weighted sum and the two masks to yield the weighted sum of one cell from each of the top- $k$  groups. This is the sparsening step. A nonlinearity is applied.

$$\mathbf{y}_{ij} = \tanh(\sigma_{ij} \cdot M_i^\lambda \cdot M_{ij}^\pi)$$

Cells that are selected are inhibited in future, mimicking the refractory period observed in biological neurons. The refractory period also ensures good utilization of all cells during training. Inhibition decays exponentially, but since we use ranking to select groups, even tiny inhibitions can have a significant effect over long periods. The period of effective inhibition depends on the number of competing groups and cells available. The hyperparameter  $0 \leq \gamma \leq 1$  determines the inhibition decay rate.

$$\phi_{ij}(t+1) = \max(\phi_{ij}(t) \cdot \gamma, \mathbf{y}_{ij})$$

Finally, we allow the option to integrate the recurrent input over time.  $\epsilon$  determines the decay rate of the integrated encoding  $\psi$ . Since the current value of  $\psi$  theoretically represents all previous states, when external input statistics are identical between training and test time,  $\epsilon$  can be zero. However, we found a generalization advantage to nonzero  $\epsilon$ , discussed later.

$$\psi(t) = \max(\psi(t-1) \cdot \epsilon, \mathbf{y})$$

$\mathbf{x}^B$  is both the recurrent input and input to any task-specific predictor or DQN networks (see experiments, below).  $\alpha$  is a normalizing scalar such that the sum of  $\mathbf{x}^B$  is 1 (since we have many zero values, and likely no negative values, other norms are inappropriate).  $\mathbf{x}^B$  is initialized as zeros and updated:

$$\mathbf{x}^B(t+1) = \alpha \cdot \psi(t)$$

The RSM layer is trained to predict the next input  $\mathbf{x}^A(t+1)$ . Prediction  $\hat{\mathbf{x}}^A$  is generated by ‘‘decoding’’ through a bottleneck of masked hidden layer group activities  $\mathbf{y}^\lambda$  by taking the max activity of the cells in each group  $i$ :

$$\mathbf{y}_i^\lambda = \max(\mathbf{y}_{i1}, \dots, \mathbf{y}_{in})$$

$w^D$  is a set of decoding weights of dimension equal to the transpose of  $w^A$ . We observed that tied weights  $w^A = (w^D)^T$  were less effective in our experiments.

$$\hat{\mathbf{x}}^A(t) = w^D \mathbf{y}^\lambda$$

The mean square error between prediction  $\hat{x}^A(t)$  and observation  $x^A(t+1)$  is minimized by stochastic gradient descent. Gradients propagate from the prediction through  $w^D$  to the sparse bottleneck  $y^\lambda$ , and subsequently to the encoding weights  $w^A$  and  $w^B$ . The latter learn to modulate hidden activity given the sequential context. We conceptualize this network as a single layer of neurons with two independently integrated dendrite trees. Max and ranking functions respectively represent local and regional competition between cells.

Training and encoding using an RSM layer only requires retention of two scalar values per cell (inhibition and recurrent input). With the exception of top-k ranking, all the functions described above are fast, simple arithmetic operations.

### 2.1. Experimental Architecture

In all our experiments we use a single RSM layer. To exploit the memory for a particular purpose, we add either a “predictor” network of two fully-connected layers, or a fully-connected Deep Q-Network (DQN) (Mnih et al., 2015) in the reinforcement learning task (see Figure 2). We use leaky-ReLU nonlinearities in these networks to reduce accumulation of dead cells due to nonstationary RSM encoding. As per our rules, gradients do not propagate from the predictor or DQN into the RSM layer. All layers are trained simultaneously & continuously using only the current input, satisfying the objective of learning using local and immediate credit assignment.

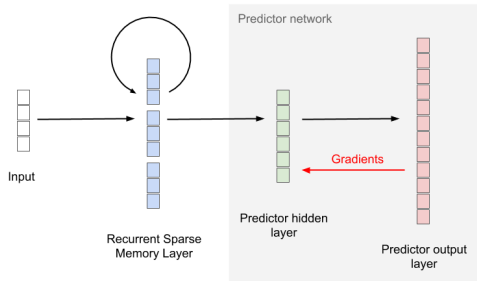


Figure 2: The architecture used in all experiments, except the reinforcement learning task where the Predictor network is replaced with a DQN. The predictor has 2 trainable layers, hidden and output. Gradients only propagate within the recurrent layer, and within the two predictor / DQN layers.

The architecture is extremely memory efficient, requiring only a single copy of previous memory state  $x^B$  and inhibition  $\phi$  in addition to current external input  $x^A$  for both training and encoding. If  $c$  is the number of cells, the asymptotic measure of RSM memory use is  $O(c)$ . Both truncated BPTT and feed-forward autoregressive approaches such as

WaveNet (Oord et al., 2016) require  $O(ct)$  where  $t$  is the time horizon.

## 3. Experiments

All experiments use the same architecture described above, with the exception that the predictor is replaced with a DQN in the maze-solving task.

Published results concerning a sparse memorization approach such as HTM (Cui et al., 2016) focus mostly on network robustness and do not enable easy comparison to more popular ANNs. We will attempt to validate the approach on a range of more easily contextualized tasks & benchmarks.

### 3.1. Associating distant cause and effect

LSTM was introduced by (Hochreiter & Schmidhuber, 1997) to solve the problem of vanishing or exploding gradients in RNNs, using gated memory cells. Hochreiter and Schmidhuber demonstrated LSTM using several example problems, including the Embedded Reber Grammar (ERG).

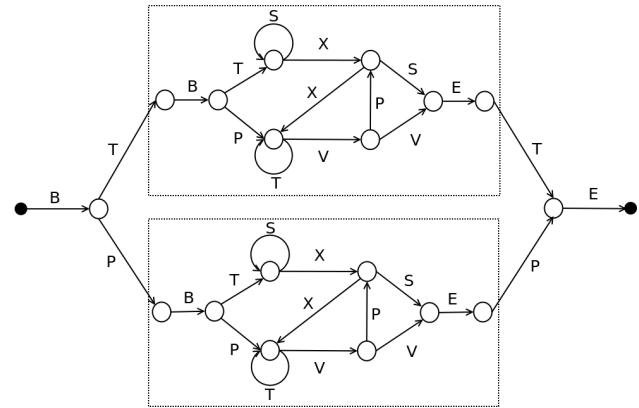


Figure 3: The Embedded Reber Grammar problem. The graph begins with a fork: B-T or B-P. The two fork paths have identical embedded ‘Reber’ grammars (dashed boxes). After a Reber grammar, T or P must be predicted correctly. The Reber grammar generates long, random, distraction sequences. Successful prediction requires the original fork to be remembered. The Recurrent Sparse Memory enables the predictor to achieve >99% accuracy.

The ERG has an initial fork (T,P), followed by the same distraction subsequence on both forks (see figure 3). The final step (T,P) can only be predicted by remembering the pre-fork symbol. For added difficulty, symbols T and P also occur in the distraction sequence. The ERG is not deterministic. It generates sequences of minimum length 9. The maximum length is unbounded, but to achieve 99% accuracy, all sequences of length  $\leq 30$  must be predicted correctly. Without gated memory cells, BPTT and RTRL fail

to solve the ERG task (Hochreiter & Schmidhuber, 1997). Cui et al report that HTM achieved 98% accuracy (Cui et al., 2016).

We believe RSM achieves high accuracy by memorizing all the sequences frequently generated by the grammar. How many must be memorized? In a sample of 5000 sequences drawn from the grammar, we observed 601 unique sequences. We used  $n = 6$  cells per group for this experiment, which implies that RSM has learned a combinatoric model to be able to memorize so many sequences.

RSM prediction is not confounded by stochastic sequences, but note that the statistics of training and test sequences are identical. Both the RSM layer and predictor components of the network achieve the same accuracy, but the predictor allows a specific label to be predicted, rather than an image of a label.

### 3.2. Modelling partially observable, higher-order sequences

We have demonstrated that RSM is able to model non-deterministic sequences, but what about sequences that are only partially observable? Since an RSM layer is easily derived from a convolutional network layer, and can handle non-deterministic sequences, it is likely RSM is able to simultaneously learn sequential and spatial structure in its input. To test this hypothesis, we presented repeating sequences of MNIST images and measured next-digit appearance & label prediction accuracy. Each step in a sequence has a specific label, and a random image of that label is selected to represent it. Due to variation in digit images, the actual sequence is only partially observable. True labels are never observed by the RSM.

Many sequences were tested, including ‘0,1,2,3,4,5,6,7,8,9’, ‘0,1,2,3,4, 0,4,3,2,1’ and ‘0,1,2,3, 0,1,2,3, 0,3,2,1’. Note that the latter are examples of higher order sequences: Correct recognition of the current image is insufficient to predict the next label.

As before, both RSM and predictor components achieved accuracy of 99%, but the predictor allows labels to be obtained. Examination of the next-image predictions is interesting - the RSM generates generic digit-image predictions (see figure 4).

When trained to classify the label of the current image, the same fully-connected predictor network achieves an accuracy of 97%. We conclude that the RSM is able to combine spatial and higher-order sequential information in a single layer to boost image classification accuracy to 99%. In many network architectures incorporating gated memory cells, a convolutional stack is used for spatial dimensionality reduction before consideration of prior state held in memory cells (for example, (Srivastava et al., 2015) uses a pretrained

stack to generate “percepts” as input to an LSTM layer). Integrated modelling of spatial and temporal data in a single layer is likely advantageous, and has been investigated (Byeon et al., 2018), but is hampered by the complexity of gated memory layers.

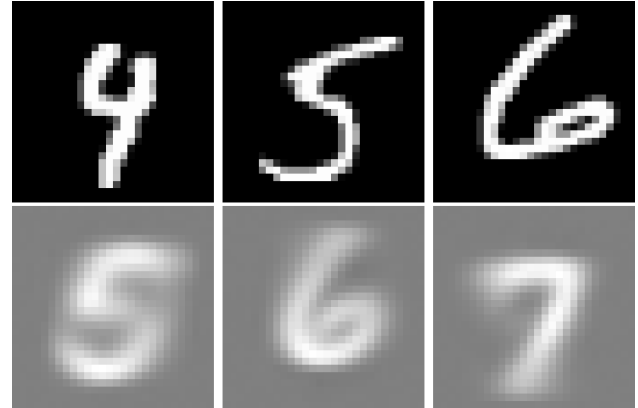


Figure 4: MNIST image sequence prediction experiment. Top row shows current images. Bottom row shows predicted images  $\hat{x}^A(t)$  given by RSM, for a sequence 0,1,...,9 repeating. Random exemplar images are selected for each instance. Note that despite the uncertain appearance of each digit, RSM is able to generate a correct “generic” digit prediction. The predictor gives the correct label prediction with >99% accuracy.

### 3.3. Deeper networks

The encoding  $x^B$  used as recurrent input can also be utilized as  $x^A$  for a deeper RSM layer. Stacking up to 3 RSM layers and using the deepest layer as predictor input did not degrade performance in our image sequence experiments, suggesting that RSM layers can be assembled into a hierarchy. In the stack, credit assignment is still local within each RSM layer. Since a single RSM layer can learn higher-order models, there is little advantage to deeper networks unless it enables more efficient dimensionality reduction, or association of multi-modal inputs.

### 3.4. Reinforcement learning with Memory

To demonstrate RSM in a reinforcement learning context, we considered the original Atari benchmarks from (Mnih et al., 2015), but in these the world is (almost) completely observable, limiting the potential benefit of a memory.

Instead, we selected an open-source 2D maze environment (Chevalier-Boisvert et al., 2018). An agent is required to navigate to the goal (see figure 5). A reward of 1.0 is provided upon reaching the goal. The agent does not know its coordinates. The agent can only observe the 3x3 cells centered at its current position, and the most recent action. The observations are individually ambiguous, so a memory

of past states and actions is needed to successfully navigate the maze.

We compared a baseline DQN agent (Mnih et al., 2015) to a DQN agent with an RSM layer. The agent architecture is most similar to the R2D2 agent (Kapturowski et al., 2019), using recurrent prioritized distributed replay.

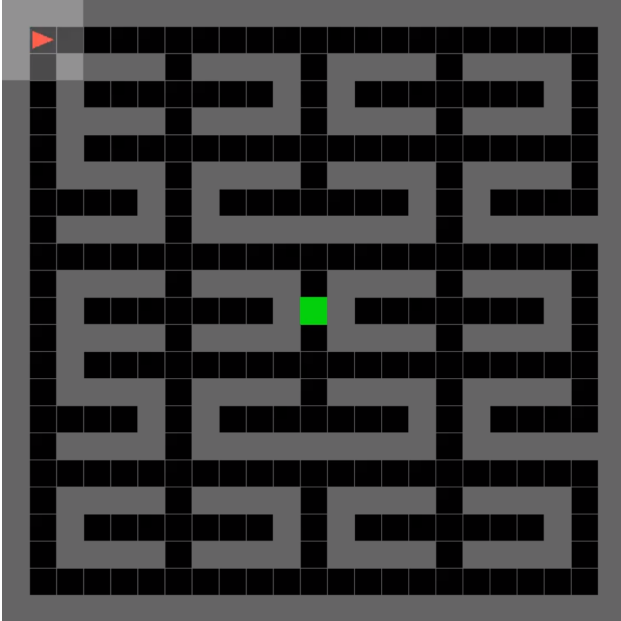


Figure 5: We compared DQN performance on a maze-navigation task with and without a RSM layer. The agent only sees a 3x3 window around itself. Here we see a maze with corridors, but an empty room was also tested. The empty room is problematic for a standard DQN because a memory of past actions is needed to keep track of agent position. Similarly, global position is ambiguous from current local sensor inputs in the corridor maze pictured. In both cases the RSM provides necessary context for the DQN to navigate successfully to the goal.

We use a two layer fully-connected variant of DQN, which then feeds into the value and advantage streams of the dueling architecture (Wang et al., 2016). The DQN hidden layers use leaky-ReLU nonlinearities.

The RSM layer is inserted between agent input and DQN sensor input, as a preprocessor, or encoder, of observations from the environment. No gradients flow between the DQN and RSM (the RSM optimizes its prediction of the next observation as described earlier). Both RSM and DQN are trained continuously and simultaneously, as the agents' behaviour evolves.

Without the RSM, the DQN is unable to solve the mazes (median reward 0 over 100 episodes). With the RSM, the agent reliably solves the mazes (median reward  $\geq 0.99$

over 100 episodes). While this result might be expected, it is interesting to confirm that the RSM can be trained in a continually evolving behavioural context and that the non-stationary RSM encoding of current and past states can be exploited by a DQN. In models using both gated memory and a DQN, gradients from the DQN propagate into the gated memory (Hausknecht & Stone, 2015; Mnih et al., 2016; Espeholt et al., 2018; Gruslys et al., 2018; Kapturowski et al., 2019). This feature is absent from our model. For all these reasons, we felt it interesting to explore compatibility between RSM and DQN.

### 3.5. Language modelling: Next word prediction perplexity

#### 3.5.1. GENERALIZATION

RSM takes the approach of remembering and encoding a long history of prior states in the current state. To achieve this, the same input in different sequential contexts generates highly orthogonal encodings. This is in contrast to gated memory layers, where a few features are *selectively* remembered, and different sequential contexts can generate similar encodings. Consequently, we anticipate that changes in sequential context between training and test datasets will severely disrupt RSM. In other words, we don't expect it to generalize well to unseen sequences.

To explore this aspect of generalization, we selected a language modelling task. The Penn TreeBank (PTB) dataset is a corpus of approximately 1 million training words and 80,000 test words. We used Mikolov's preprocessing (Mikolov et al., 2011), which results in a dictionary of 10,000 unique words. PTB is known to present a difficult generalization challenge due to the small size of the corpus. Next-word prediction quality is typically measured using perplexity (PPL). Model output is a distribution over the words in the dictionary.

#### 3.5.2. GENERALIZATION FEATURES

For RSM, even small changes between training and test sequences can be disruptive. Imagine that the training corpus contains 'The cat sat on the mat' and the test corpus 'The cat sat on a mat'. Although the RSM encoding would be identical until 'on', subsequent states would be highly orthogonal, so the predictor cannot predict 'mat' from combinations of active cells never previously observed. To mitigate these types of generalization error, we enabled some minor features.

First, we integrate feedback to the RSM using  $\epsilon > 0$ . This is not needed to help RSM learn sequences, but it does help RSM *generalize* learned sequences. We apply dropout at rate 0.5 to encourage the RSM to make use of earlier encodings, for example the active cells representing 'The

cat sat’ are all predictive of a future ‘mat’. Second, we provide the integrated RSM state to the predictor. These changes reduce test perplexity by 10-15.

The third change is to “forget” the recurrent state of the network with a fixed probability  $\mu$  during training. If forgetting is randomly selected, we set integrated activity  $\psi$  and inhibition  $\phi$  to zeros. The intention is to expose the predictor to different subsequences, in effect augmenting the training set. This feature improves test perplexity by another 5-10 points.

### 3.5.3. REGULARIZATION

We attempted to regularize the RSM and predictor networks via conventional techniques - in particular adding an L2 loss term, and dropout. We found neither helpful when added to the RSM, but a small L2 value improved predictor performance.

To understand why these techniques are ineffective with this architecture, consider (Cui et al., 2016), which was one of the inspirations for our work. They show that sparse distributed representations are extremely robust to network damage, because the meaning of individual elements is correlated. Therefore, to successfully “ignore” features, many cells’ activity must be simultaneously excluded. This is difficult for reasonable levels of both dropout and weight penalties. So it seems ineffective regularization may be a consequence of distributed representations that are robust to damage.

### 3.5.4. MODEL INTERPOLATION

(Mikolov et al., 2011) showed that linear interpolation of model distributions to produce ensemble predictions - a form of smoothing - is very often effective at reducing test perplexity. In particular, earlier RNN and LSTM language models (which we are using as a baseline) were often presented as ensembles. 5-gram language models with Kneser-Ney smoothing (KN5) (Chen & Goodman, 1999) are optimal for the PTB corpus; higher n-gram models do not deliver better test perplexity.

When a word occurs, it is likely to occur again in the near future. This general principle leads to cache language models. (Mikolov et al., 2011) also showed that caches invariably improve ensemble perplexity. We felt that adding a fixed, exponentially-decaying probability mass to words after observation - a primitive cache - meets our biological plausibility criteria. We did not allow ‘adaptive’ modelling (i.e. allowing the RSM to learn during the test). We report RSM results interpolated with the simplistic cache, and optionally with KN5 for easier comparison and insights on n-gram ensemble complementarity.

### 3.5.5. RESULTS

With  $m = 600$  groups,  $k = 20$ ,  $n = 6$  cells per group and 4 epochs of training with batch size 300, we obtained 50% next word prediction accuracy and a perplexity of 9 on the training corpus. Training perplexity and accuracy had not plateaued. This suggests that moderately sized RSM layers can memorize extremely long sequences.

We found test perplexity to be better with  $n = 8$  cells per group and only 0.25 epochs of training (see table 1). We observed next word prediction accuracy of 20.6% on the test corpus. Accuracy is rarely reported for language models, but in our case it is interesting because we obtained good accuracy but poor perplexity. RSM per-word perplexity is bi-modal, showing rapid oscillations between very low and high values. When not combined with KN5, a small uniform mass significantly reduces average RSM test perplexity (reported result without KN5 includes 7% uniform mass).

Model	Test PPL
RSM	166
KN5	143
RSM+KN5	124

Table 1: Test perplexity of RSM model, KN5, and both combined.

RSM + KN5 test perplexity is significantly lower than either RSM or KN5 alone. The complementarity suggests that RSM exploits more context than KN5, context that can only sometimes be exploited.

To put these results in context, (Mikolov et al., 2010) reports next-word perplexity using a simple RNN, like RSM, but without sparse coding and inhibition to capture higher order sequences. They also interpolate with KN5. On the Wall St. Journal (WSJ) dataset they obtained 225 PPL when training on 1 million words (similar to PTB corpus size) and 156 when training with 6.4 million words.

(Mikolov et al., 2011) helpfully benchmarks many methods on PTB. RSM is comparable to several early methods such as 5-gram Good-Turing, Random Clusterings, Random Forest and 5-gram Maximum Entropy, both individually and interpolated with KN5. RNNs trained with short-context BPTT are significantly better than RSM, with PPL 124 (RNN) and 105 (RNN+KN5).

Careful regularization of modern gated-memory ANN language models such as LSTM reduces PTB test PPL from 124 to 100 or less (Zaremba et al., 2014), with state of the art scores < 60 (Merity et al., 2017).

Overall, RSM test PPL is comparable to early language models, slightly better than simple RNNs, and significantly



---

worse than modern ANN architectures like LSTM.

## 4. Summary

We showed that RSM can successfully learn to exploit distant causes when predicting later effects, or in the reinforcement learning context, when choosing appropriate actions. RSM can learn higher-order sequences, likely with combinatoric representational efficiency, despite some degree of uncertainty and partial observability.

RSM has a number of advantages - an order of magnitude reduction in memory requirements, very large memory capacity, batch-online training, and it is not necessary to specify the maximum time horizon in advance. For complex sequence learning tasks with similar training and test statistics, the RSM approach is appealing due to its simplicity and speed. However, although stochastic processes are not confounding, generalization to *unseen* test sequences is clearly limited. In a language modelling task, when longer context is unnecessary, and training data is limited, this is a significant drawback.

In the image sequence prediction task, RSM was continually exposed to unseen sequences of observations due to the large number of images of each digit. Why was this form of generalization not pathological? First, we believe that RSM is able to perform spatial generalization as well as any other two-layer convolutional network; it is only unseen sequence generalization that is limited. Second, it is not possible to memorize the infinite observed training sequences, and the training regime therefore forces RSM to learn a generalized sequence model.

### 4.1. Selective remembering

We expect that RSM would perform better as a language model given a larger training corpus, but would that merely be masking a fundamental weakness?

One of the most significant differences between RSM and gated memory layers is the strategy of “remember everything” versus “selectively remember useful things”. The latter approach is able to generalize better, because it is not distracted by irrelevant features in unseen test data.

Recent work has shown that self-attention is a very effective mechanism for selecting useful features from sequences (Vaswani et al., 2017), with groundbreaking results in neural language models. (Radford et al., 2019) uses self-attention in an unsupervised next-word-prediction training regime, like RSM, but autoregressive feed-forward rather than recurrent. In future work we will attempt to use self-attention to selectively remember sequences using RSM, without violating our biological plausibility constraints.

## Acknowledgments

Thanks to Alan Zhang, for conversations about the nature of generalization and learning representations.

### Author Contributions

DR and GK devised the concept and experiments. AA, DR and GK wrote the code. DR and AA executed the experiments. DR, AA and GK wrote the paper.

## References

- Bai, Shaojie, Kolter, J Zico, and Koltun, Vladlen. An empirical evaluation of generic convolutional and recurrent networks for sequence modeling. *arXiv preprint arXiv:1803.01271*, 2018.
- Balduzzi, David, Vanchinathan, Hastagiri, and Buhmann, Joachim. Kickback cuts backprop’s red-tape: biologically plausible credit assignment in neural networks. In *Twenty-Ninth AAAI Conference on Artificial Intelligence*, 2015.
- Bengio, Yoshua, Lee, Dong-Hyun, Bornschein, Jorg, Mesnard, Thomas, and Lin, Zhouhan. Towards biologically plausible deep learning. *arXiv preprint arXiv:1502.04156*, 2015.
- Byeon, Wonmin, Wang, Qin, Kumar Srivastava, Rupesh, and Koumoutsakos, Petros. Contextvp: Fully context-aware video prediction. In *Proceedings of the European Conference on Computer Vision (ECCV)*, 2018.
- Chelba, Ciprian, Mikolov, Tomas, Schuster, Mike, Ge, Qi, Brants, Thorsten, Koehn, Phillipp, and Robinson, Tony. One billion word benchmark for measuring progress in statistical language modeling. *arXiv preprint arXiv:1312.3005*, 2013.
- Chen, Stanley F and Goodman, Joshua. An empirical study of smoothing techniques for language modeling. *Computer Speech & Language*, 13(4):359–394, 1999.
- Chevalier-Boisvert, Maxime, Willems, Lucas, and Pal, Suman. Minimalistic gridworld environment for openai gym. <https://github.com/maximecb/gym-minigrid>, 2018.
- Chung, Junyoung, Gulcehre, Caglar, Cho, KyungHyun, and Bengio, Yoshua. Empirical evaluation of gated recurrent neural networks on sequence modeling. *arXiv preprint arXiv:1412.3555*, 2014.
- Cui, Yuwei, Ahmad, Subutai, and Hawkins, Jeff. Continuous Online Sequence Learning with an Unsupervised Neural Network Model. *Neural computation*, 28:2474–2504, 2016.



- 
- Espeholt, Lasse, Soyer, Hubert, Munos, Remi, Simonyan, Karen, Mnih, Vlad, Ward, Tom, Doron, Yotam, Firoiu, Vlad, Harley, Tim, Dunning, Iain, Legg, Shane, and Kavukcuoglu, Koray. IMPALA: Scalable distributed deep-RL with importance weighted actor-learner architectures. In Dy, Jennifer and Krause, Andreas (eds.), *Proceedings of the 35th International Conference on Machine Learning*, volume 80 of *Proceedings of Machine Learning Research*, Stockholmmsässan, Stockholm Sweden, 2018. PMLR.
- Gruslys, Audrunas, Dabney, Will, Azar, Mohammad Gheshlaghi, Piot, Bilal, Bellemare, Marc, and Munos, Remi. The reactor: A fast and sample-efficient actor-critic agent for reinforcement learning. In *International Conference on Learning Representations*, 2018.
- Guerguiev, Jordan, Lillicrap, Timothy P, and Richards, Blake A. Towards deep learning with segregated dendrites. *ELife*, 6:e22901, 2017.
- Hausknecht, Matthew J. and Stone, Peter. Deep recurrent q-learning for partially observable mdps. *CoRR*, abs/1507.06527, 2015.
- Hawkins, Jeff and Ahmad, Subutai. Why neurons have thousands of synapses, a theory of sequence memory in neocortex. *Frontiers in neural circuits*, 10:23, 2016.
- Hochreiter, Sepp and Schmidhuber, Jürgen. Long short-term memory. *Neural computation*, 9(8):1735–1780, 1997.
- Kapturowski, Steven, Ostrovski, Georg, Dabney, Will, Quan, John, and Munos, Remi. Recurrent experience replay in distributed reinforcement learning. In *International Conference on Learning Representations*, 2019.
- Khemlani, Sangeet Suresh, Mackiewicz, Robert, Bucciarelli, Monica, and Johnson-Laird, Philip N. Kinematic mental simulations in abduction and deduction. *Proceedings of the National Academy of Sciences*, 110(42):16766–16771, 2013.
- Luo, Hongyin, Fu, Jie, and Glass, James. Adaptive bidirectional backpropagation: Towards biologically plausible error signal transmission in neural networks. *arXiv preprint arXiv:1702.07097*, 2017.
- Makhzani, Alireza and Frey, Brendan. K-sparse autoencoders. *arXiv preprint arXiv:1312.5663*, 2013.
- Makhzani, Alireza and Frey, Brendan J. Winner-Take-All Autoencoders. In *Advances in Neural Information Processing Systems*, 2015.
- Merity, Stephen, Keskar, Nitish Shirish, and Socher, Richard. Regularizing and optimizing lstm language models. *arXiv preprint arXiv:1708.02182*, 2017.
- Mikolov, Tomáš, Karafiát, Martin, Burget, Lukáš, Černocký, Jan, and Khudanpur, Sanjeev. Recurrent neural network based language model. In *Eleventh annual conference of the international speech communication association*, 2010.
- Mikolov, Tomáš, Deoras, Anoop, Kombrink, Stefan, Burget, Lukáš, and Černocký, Jan. Empirical evaluation and combination of advanced language modeling techniques. In *Twelfth Annual Conference of the International Speech Communication Association*, 2011.
- Mnih, Volodymyr, Kavukcuoglu, Koray, Silver, David, Rusu, Andrei A, Veness, Joel, Bellemare, Marc G, Graves, Alex, Riedmiller, Martin, Fidjeland, Andreas K, Ostrovski, Georg, et al. Human-level control through deep reinforcement learning. *Nature*, 518(7540):529, 2015.
- Mnih, Volodymyr, Badia, Adria Puigdomenech, Mirza, Mehdi, Graves, Alex, Lillicrap, Timothy, Harley, Tim, Silver, David, and Kavukcuoglu, Koray. Asynchronous methods for deep reinforcement learning. In Balcan, Maria Florina and Weinberger, Kilian Q. (eds.), *Proceedings of The 33rd International Conference on Machine Learning*, volume 48 of *Proceedings of Machine Learning Research*, New York, New York, USA, 2016. PMLR.
- Ney, Hermann, Essen, Ute, and Kneser, Reinhard. On structuring probabilistic dependences in stochastic language modelling. *Computer Speech & Language*, 8(1):1–38, 1994.
- Olshausen, Bruno A and Field, David J. Sparse coding with an overcomplete basis set: A strategy employed by v1? *Vision research*, 37(23):3311–3325, 1997.
- Oord, Aaron van den, Dieleman, Sander, Zen, Heiga, Simonyan, Karen, Vinyals, Oriol, Graves, Alex, Kalchbrenner, Nal, Senior, Andrew, and Kavukcuoglu, Koray. Wavenet: A generative model for raw audio. *arXiv preprint arXiv:1609.03499*, 2016.
- O’Reilly, Randall C. Biologically plausible error-driven learning using local activation differences: The generalized recirculation algorithm. *Neural computation*, 8(5): 895–938, 1996.
- Radford, Alec, Wu, Jeffrey, Child, Rewon, Luan, David, Amodei, Dario, and Sutskever, Ilya. Language models are unsupervised multitask learners. *OpenAI Blog*, 1:8, 2019.
- Srivastava, Nitish, Mansimov, Elman, and Salakhutdinov, Ruslan. Unsupervised learning of video representations using lstms. *arXiv preprint arXiv:1502.04681*, 2015.
- Sutskever, Ilya. *Training recurrent neural networks*. University of Toronto Toronto, Ontario, Canada, 2013.

---

Vaswani, Ashish, Shazeer, Noam, Parmar, Niki, Uszkoreit, Jakob, Jones, Llion, Gomez, Aidan N., Kaiser, Lukasz, and Polosukhin, Illia. Attention Is All You Need. (Nips), 2017.

Wang, Ziyu, Schaul, Tom, Hessel, Matteo, Van Hasselt, Hado, Lanctot, Marc, and De Freitas, Nando. Dueling network architectures for deep reinforcement learning. In *Proceedings of the 33rd International Conference on International Conference on Machine Learning - Volume 48*, ICML'16. JMLR.org, 2016.

Williams, Ronald J and Zipser, David. Gradient-based learning algorithms for recurrent. *Backpropagation: Theory, architectures, and applications*, 433, 1995.

Zaremba, Wojciech, Sutskever, Ilya, and Vinyals, Oriol. Recurrent neural network regularization. *arXiv preprint arXiv:1409.2329*, 2014.

---

## A. Appendix

### A.1. Hyperparameters

The following values were used in our experiments. A learning rate of 0.0005 was used with the Adam optimizer in all experiments.

<b>Distant Cause &amp; Effect</b>	
$m$ (groups)	200
$n$ (cells per group)	6
$k$ (sparsity)	25
$\gamma$ (inhibition decay rate)	0.98
$\epsilon$ (recurrent input decay rate)	0
Batch size	400
Predictor hidden layer size	500
<b>Partially Observable Sequences</b>	
$m$ (groups)	200
$n$ (cells per group)	6
$k$ (sparsity)	25
$\gamma$ (inhibition decay rate)	0.5
$\epsilon$ (recurrent input decay rate)	0
Batch size	300
Predictor hidden layer size	1200
<b>Reinforcement Learning with Memory</b>	
$m$ (groups)	200
$n$ (cells per group)	8
$k$ (sparsity)	20
$\gamma$ (inhibition decay rate)	0.95
$\epsilon$ (recurrent input decay rate)	0
Batch size	100
DQN hidden layer sizes	500, 500
<b>Language Modelling</b>	
$m$ (groups)	600
$n$ (cells per group)	8
$k$ (sparsity)	20
$\gamma$ (inhibition decay rate)	0.8
$\epsilon$ (recurrent input decay rate)	0.85
Batch size	300
Predictor hidden layer size	1200

Table 2: Hyperparameter values for reported experiments